Assessment of industrial waste for adsorption and capture of CO_2: Dynamic and static capture system

Pamela B. Ramos, Marcelo F. Ponce, Florencia Jerez, Gastón P. Barreto, Marcela A. Bavio

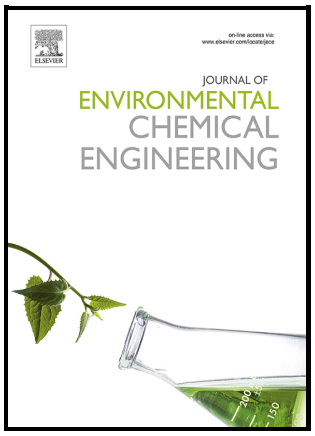

PII: S2213-3437(22)00394-3

DOI: https://doi.org/10.1016/j.jece.2022.107521

Reference: JECE107521

To appear in: *Journal of Environmental Chemical Engineering*

Received date: 27 October 2021
Revised date: 23 February 2022
Accepted date: 5 March 2022

Please cite this article as: Pamela B. Ramos, Marcelo F. Ponce, Florencia Jerez, Gastón P. Barreto and Marcela A. Bavio, Assessment of industrial waste for adsorption and capture of CO_2: Dynamic and static capture system, *Journal of Environmental Chemical Engineering,* (2021) doi:https://doi.org/10.1016/j.jece.2022.107521

Assessment of industrial waste for adsorption and capture of CO_2: Dynamic and static capture system

Pamela B. Ramos [a, b]*, Marcelo F. Ponce [a, c], Florencia Jerez [a, c], Gastón P. Barreto [a, b], Marcela A. Bavio [a, c],

[a] *Dto. Ingeniería Química y Tecnología de los Alimentos, Facultad de Ingeniería, UNCPBA, Avda. del Valle 5737, B7400JWI, Olavarría, Buenos Aires, Argentina*

[b] *INMAT. CIFICEN (CICPBA-CONICET-UNCPBA), Argentina.*

[c] *INTELYMEC. CIFICEN (CICPBA-CONICET-UNCPBA), Argentina.*

**E-mail address (author): pamela.ramos@fio.unicen.edu.ar*

Tel: +54 02284-451055 int. 277

Abstract

The increasing generation and accumulation of waste derived from production and consumption activities constitute a severe social and environmental problem. Industrial waste from the glass industry, with SiO_2 (WSi) and Al_2O_3 (WAl) high content, were studied as materials for CO_2 capture in stationary and dynamic systems. These were characterized by Scanning Electron Microscopy (SEM) and Energy Dispersive X-ray spectroscopy (EDX), N_2 adsorption-desorption isotherms accompanied BET (Brunauer-Emmett-Teller) analysis, X-ray diffraction (XRD), and Fourier Transform Infrared Spectroscopy (FTIR). Adsorbed CO_2 (mmol) was measured using the gas measurement

technique in FTIR. In all tests, the WSi residue had a higher adsorption capacity than the WAl. The adsorption capacity obtained was 0.97 mmol CO_2 g^{-1} at 20°C and 16% CO_2 in a dynamic system for WSi. The effect of temperature and CO_2 concentration on the retention capacity of both wastes was analyzed. Three models were used to evaluate the kinetic behaviour as a function of the temperature of the test. The results indicate that under conditions of 16% vol CO_2 and 20ºC, the pseudo-first order model is the one that best fits. The saturation time of the materials was around 10 minutes. Simulated CO_2 streams and real gas samples were tested. Real gas samples were extracted from gaseous streams from the combustion of flour mill and beer wastes production. CO_2 retention is evidenced; however, the capture capacity was higher in WSi, about 63%, compared to 30% for WAl. The wastes have good efficiency in the CO_2 capture and high yield in the successive uses. The application of these waste materials for CO_2 capture provides advantages in terms of decrease waste pretreatment costs, a technological solution for the disposal of the abundant glass industry residue, efficient CO_2 capture under different conditions and an approximation to use in real systems.

Keywords: Carbon dioxide, capture system, solid waste, environmental.

1. Introduction

Within the general problem of Climate Change in the world, undoubtedly among the most harmful factors for the ecosystems is air pollution, where the emission and capture of Greenhouse Gases (GHG) as CO_2, CH_4, NO_X, SO_X have considerable importance [1]. Since the Industrial Revolution, anthropic activities linked to the burning of fossil fuels, industrial processes, and urban waste generation have multiplied exponentially. This has produced and

continues to make persistent anthropogenic changes that cause greenhouse gas concentrations in the atmosphere to rise above natural levels, thus increasing the greenhouse effect and causing climate change. The World Meteorological Organization reported in 2018 that CO_2 concentration reached globally averaged 407.8 ppm, presenting a new world record and an increase from the pre-industrial era of about 147% [2]. In 2017, the Ministry of Environment and Sustainable Development of Argentina published the National Inventory of Greenhouse Gases (GHG), which revealed that Argentina contributed in 2014 a total of 368.3 $MtCO_2eq$, corresponding to 0.7% of global emissions [3].

The sector with the highest contribution to emissions corresponds to the agriculture, livestock, and deforestation sector, with a 39% share. The energy sector is another of the most relevant and contributes 53% of total emissions [4]. Due to the magnitude of global and local CO_2 emissions, there are critical points concerning the development of potential capture technologies, adsorbent materials, and regeneration modes.

CO_2 capture and storage (CCS) are considered a technological alternative to include in the ways of reducing CO_2 emissions. Currently, there is a growing interest in adsorption-based post-combustion CO_2 capture due to its energy reduction potential and the possibility of integration with existing industrial plants with low cost and easy retrofitting. In addition, this technology presents the flexibility to capture CO_2 from different industrial sources due to its different modes of regeneration of sorbents and types of reactors [5, 6]. Several types of reactor configurations are used for CO_2 capture. These include conventional fixed bed, structured fixed bed, moving bed, conventional fluidized bed, and multi-stage fluidized bed. Although the choice of the most suitable reactor configuration is an essential factor in real post-combustion processes. Also, the mode of regeneration affects the process, which should

be efficient and, simultaneously, cost-effective to industrial scale [5-7]. Different regeneration modes are suitable in industrial plants. The vacuum swing regeneration (VSA) was proved to be the best against temperature swing (TSA), which causes very long cycle times due to the heat transfer limitation in heating and cooling. However, VSA is impractical on an industrial scale since it requires the use of a two-stage vacuum oscillation adsorption system that increases costs and complexity. Pressure swing adsorption (PSA) is widely used in the industrial sector. However, it holds significant disadvantages when used in post-combustion capture applications due to the flue gases emitted at atmospheric pressure with a relatively low CO_2 concentration (<20 %vol). In order to overcome the drawbacks of the different modes of regeneration, hybrid strategies emerged; thus, a hybrid vacuum temperature swing adsorption (VTSA), combining VSA and TSA and, hybrid vacuum pressure swing adsorption (VPSA), connecting VSA and PSA have been implemented in different combinations of reactors [5-8].

On the other hand, many promising new materials to capture gaseous pollutants have been developed [9-11]. The sorbent characteristics in the CO_2 capture system determine the competitiveness of the adsorption technology [12]. Desirable materials for CO_2 capture should have good adsorption performance in equilibrium and at low CO_2 pressure (<0,2 atm [12]), particle size <2000 μm (depending on reactor configuration), selectivity in humid conditions, stability in cyclic operation, fast adsorption/desorption kinetics, low cost, low energy requirements and, scalability [12, 13]. Due to their surface characteristics, adsorbent materials based on carbon [14-16], zeolites [17-19], metallic organic frameworks (MOFs) [20, 21], metal oxides [22], among others [23, 24], have been studied. Zeolite-based materials have poor selectivity in humid conditions, carbon-based materials have

poor selectivity in CO_2/N_2 mixtures, and MOFs materials are expensive. Due to these disadvantages, their high energy requirement in the regeneration process and synthesis costs affect its scalability [13]. Also, as far as absorption technologies based on amine aqueous solutions are concerned, they have been widely used industrially for 50 years to capture CO_2 after combustion [25, 26]. However, they have high energy requirements for regeneration and provoke equipment corrosion and chemical degradation [27]. In recent years, research efforts have focused on finding solutions by substituting traditional solvents such as MEA for systems with aqueous mixtures of amines containing DMCA, MAP, CHAP with promising results showing a decrease in energy costs by reducing the temperature of the regeneration process [28, 29]. In turn, aqueous amines immobilized in mesoporous silica matrices have attracted considerable attention due to their high efficiency and selectivity for CO_2 capture of a gas mixture [30].

Due to the weaknesses of the adsorbent materials mentioned above, it is necessary to continue searching for new CO_2 capture materials. The recovery of residues produced by various industries can be a promising alternative to lower the manufacturing costs of adsorbents and the energy requirements and give technological disposal of waste and insert them back into the production circle. Several materials using mesoporous silica have been investigated as their structural characteristics are critical for their performance as adsorbent materials [31-34]. However, it is still a material that needs a wide variety of chemical precursors, high energy costs for its production, and superficial modification to increase its efficiency [35, 36]. Moreover, some investigations seek to reduce the environmental effects and the costs of producing these oxides by modifying the synthesis methods, replacing some chemical precursors with others that are more environmentally friendly. This study's novelty

lies in using two industrial wastes that contain silica and aluminum oxides instead of a synthetic material to capture CO_2. These wastes are abundant residues of the polishing and finishing of glass industry. In this way, the energy and environmental cost of synthesizing the adsorbent material can be eliminated through residue properties analysis, adsorption capacity study, and the evaluation of the reuse cycles.

In this context, the main aim of the current study is to assess the CO_2 adsorption capacity of waste materials from the glass industry. This work has two major goals: reducing atmospheric pollution and reusing/recovering industrial waste. These will be reached using valorized materials in an environment-friendly application, with low cost, easy and inexpensive large-scale production, and minimal energy requirements. Accomplishing this is of paramount importance in this consumer society, and it is essential for protecting present and future generations. The residues were characterized, applied in consecutive adsorption cycles and its reuse efficiency for CO_2 capture was evaluated in both wastes. The behaviour of the system at different temperatures was analyzed. In addition to the simulated systems tests, measurements were made with real samples taken from the flue gases in coal production.

2. Experimental

2.1. Materials and characterization

The waste samples used in this experimental study come from a company dedicated to manufacturing double-glazed, tempered, laminated ~~glass~~, and ground glasses located in Olavarría, Buenos Aires, Argentina. The first waste was collected from the polishing process of monolithic and laminated glass (WSi), and the second was extracted from the grinding process of monolithic glass (WAl). Samples were collected for one week and

homogenized. They were dried for 1 h at 90 °C on a stove to remove all moisture from the residue. Later, they were morterized in a mill to unify and homogenize the particle size.

WSi and WAl were characterized by SEM/EDX (FESEM-FEI Inspect F50 microscope) to determine morphological characteristics and surface composition. Nitrogen adsorption-desorption isotherms were made using the equipment Micromeritics ASAP 2420 NSP. The surface area was determined by the BET (Brunauer-Emmett-Teller) equation; pores size and volume distribution were determined using the BJH (Barett-Joyner-Halenda) method. XRD patterns of the waste were obtained on a PANalytical Empyrean diffractometer, using CuKa (λ= 1.54 Å) radiation and a PIXcel3D detector. Infrared spectra of the samples were obtained employing an FTIR Nicolet, Magna 550, with CsI optics, after preparing KBr pellets.

2.2. Quantification of CO_2 by FTIR

The measurement of CO_2 fraction was carried out using the FTIR (Nicolet Magna 500) and its gas cell with a volume of 39 cm^3 and 100 mm in length. The background and spectrum were obtained using 100 scans with a resolution of 4 cm^{-1}. Before each measurement, the cell was cleaned with N_2 to remove any adsorbed substance. The calibration curve was performed with a mixture of CO_2 and N_2 with a concentration range of CO_2 between 0-12% v/v. The CO_2 could be quantified by performing a calibration curve calculating the band's area with the highest intensity for carbon dioxide, 2414 cm^{-1} - 2198 cm^{-1}.

Figure 1a) shows the different spectra of CO_2 present in gaseous samples of known CO_2/N_2 concentration. A reduction can be observed in the areas under the curve of the characteristic peaks corresponding to the different CO_2 concentrations. The calibration curve (Figure 1b))

was constructed from the extraction of samples from a dynamic system under a CO_2/N_2 stream of 330 mL min^{-1} (R^2=0.986). To measure high concentrations of CO_2 (greater than 12%), a smaller sample volume is placed inside the cell, and the final book is maintained by adding nitrogen. Using the calibration curve, the CO_2 not adsorbed on the solid is obtained.

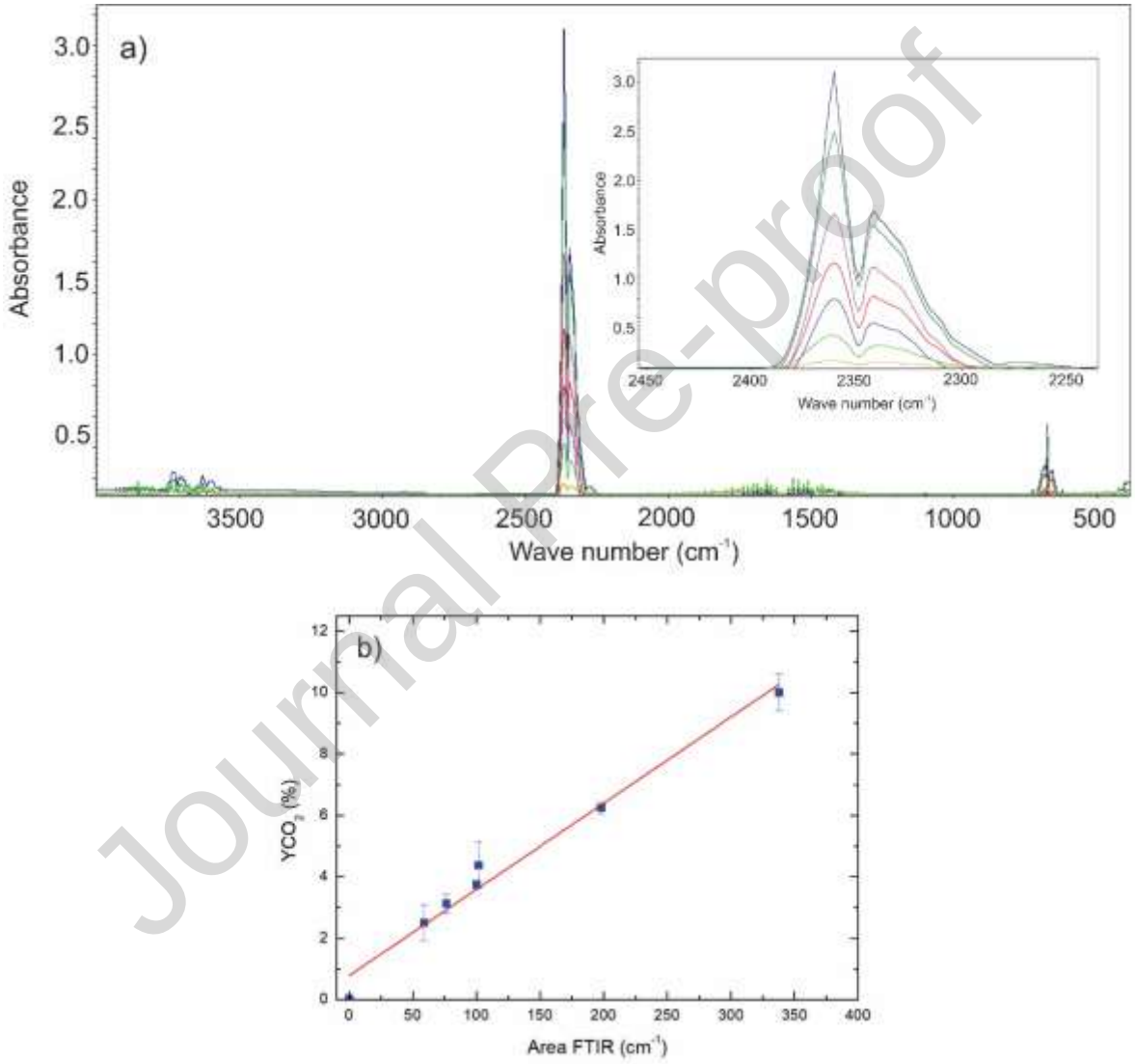

Figure 1. a) FTIR spectrum of the different CO_2 concentrations during calibration analysis, **b)** calibration curve for CO_2 vs. area (bands 2414 cm^{-1}- 2198 cm^{-1}).

2.3. Experimental Methodology of CO_2 adsorption

2.3.1. CO_2 capture: Static system

Adsorption experiments were carried out by contacting a known volume of a mixture of CO_2 and N_2 with a bed containing a known amount of WSi or WAl. Initially, the wastes were heated to 110°C in a nitrogen atmosphere (99.8%) under a flow of 4 L min^{-1} for 60 min and then left cooled to room temperature under a nitrogen atmosphere to remove the water content and other species adsorbed on the surface [37]. Next, 250 mg of the waste (WSi or WAl) was placed in an adsorption bed of 3 cm, where it was exposed to different contact times with 25 cm^3 of a mixture of gases at atmospheric pressure, with an initial concentration of 10%, 16%, 24% and 50% of CO_2 in N_2 at *ca.* 20°C. After the contact time (from 1 min to 60 min, at intervals of 1 min), the gaseous sample was placed in the gas cell, to which sufficient vacuum was previously made (30 mmHg). Then the measurement of CO_2 not adsorbed was quantified by FTIR.

Figure 2 shows the diagram for the CO_2 capture tests. For the static system, valve 1 is opened, valves 2 and 3 are kept closed, the chamber is filled, and valve 1 is subsequently closed. Then valve 2 is opened and left for an exposure time with the adsorbent material, and it is closed. With all the valves closed, the chamber is removed. Finally, to measure the amount of CO_2 adsorbed, the FTIR gas cell is evacuated, and the sample is placed in it to be measured.

The waste stability was evaluated by reuse cycles. After 60 minutes of contact, the system was heated to 100°C for 1 hour in an N_2 atmosphere, removing the adsorbed CO_2; it was allowed to cool to room temperature and placed back in contact with CO_2, this process was repeated 5 consecutive times.

2.3.2. CO_2 capture: Dynamic system

Adsorption experiments were carried out by passing a stream of CO_2/N_2 through a U-shaped glass tube that contained a known amount of WSi and WAl (adsorptive waste bed). The CO_2 concentration of the stream before and after adsorption was calculated using an infrared gas cell by FTIR. Adsorption tests were performed at atmospheric pressure.

The initial treatment is the same as that described for trials in static capture systems. A known amount of WSi and WAl was placed in a bed and flows of 330 mL min^{-1}, and 660 mL min^{-1} [38] were circulated, with initial concentrations of 10%, 16%, 24%, and 50% vol CO_2 in N_2 at different temperatures. The flow rate is constant during CO_2 adsorption test. The adsorption test begins after 3 minutes to stabilize the gas system. At the exit, the CO_2/N_2 samples were taken every 1 minute and measured at FTIR as in section 2.3.1.

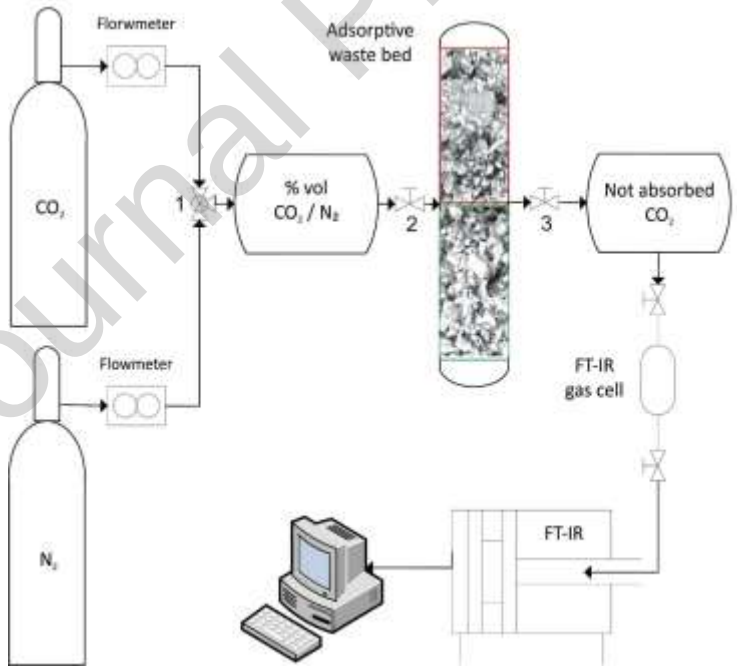

Figure 2. Diagram of the static and dynamic systems for CO_2 adsorption testing and waste disposition in the systems.

The amount of CO_2 (mmol) adsorbed per gram of solid when the tests are carried out in a dynamic system was obtained using the calibration curve and Equation (1). Where Q is the flow of CO_2 (L min^{-1}), W is the weight of the adsorbent solid in g, C_0 and C_f are the concentrations of CO_2 (mmol L^{-1}) at time 0 and final time (60 min).

$$\frac{mmol\ CO_2}{g\ solid} = Qx\frac{\int_0^t (C_0 - C_f)\ dt}{W} \quad (1)$$

The experimental results obtained at different temperatures were adjusted to the kinetics of pseudo-first order, pseudo-second order, and Avrami [39] to evaluate the effect of temperature on the kinetics of CO_2 adsorption. The equations of the kinetic models for CO_2 adsorption and their characteristic parameters from the following equation (2), (3) and (4):

Pseudo-first order: $\frac{d_{qe}}{dt} = k_f(q_e - q_t)$ (2)

Pseudo-second order: $\frac{d_{qe}}{dt} = k_L t\ (q_e - q_t)^2$ (3)

Avrami model: $\frac{d_{qe}}{d_t} = k_A^{n_A}\ t^{n_A - 1}\ (q_e - q_t)$ (4)

where q_e y q_t indicates the adsorption amount of the sample in equilibrium and at time t. k_f, k_s and k_A are the adsorption rate constants, and n_A is a constant of the Avrami model.

3. Results and discussion

3.1. Wastes characterization

Figure 3 shows WSi and WAl micrographs at 10.000x magnification and 20 kV acceleration voltage. Both wastes have a heterogeneous distribution of particle size, with a

granulometry of 238.42 μm (90%) to 153.29 μm (50%) for WSi, and 445.12 μm (90%) to 118.18 μm (50%) for WAl. Also, non-porous surfaces were observed at magnifications of 1500x. However, plate-like particles are observed, which could lead to porosity within the laminar plates.

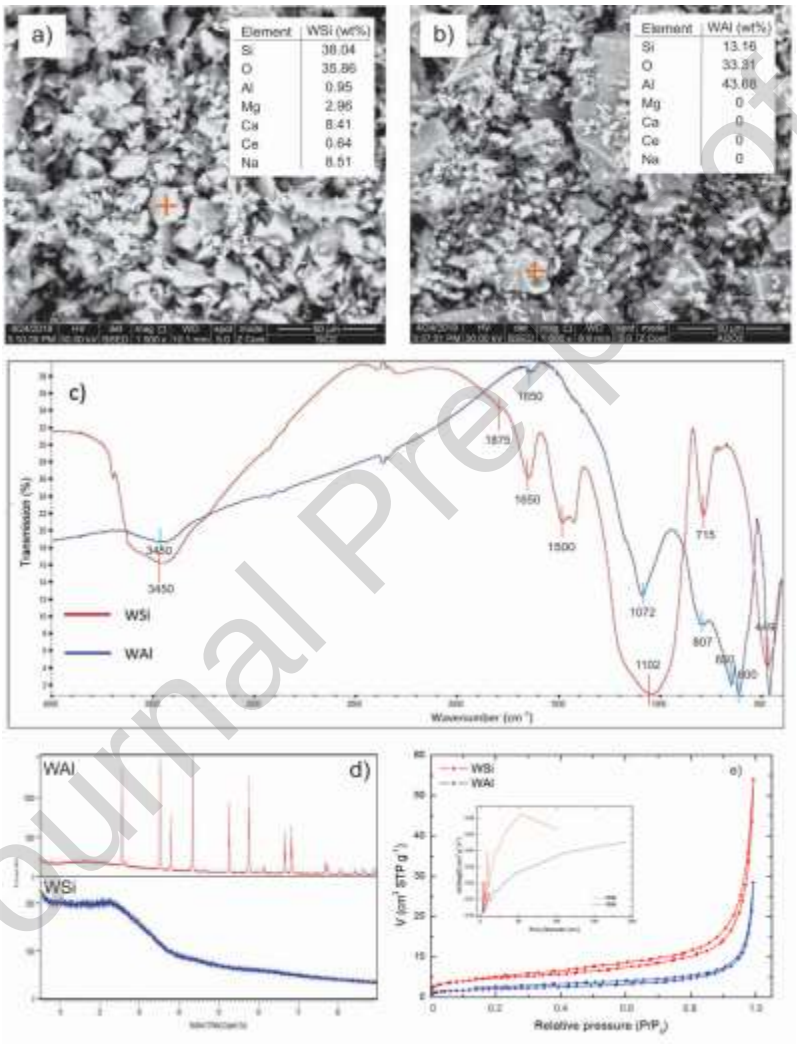

Figure 3. Wastes characterization: SEM micrographs and EDX analysis of waste **a)** WSi and **b)** WAl, **c)** FTIR spectra of WSi and WAl, **d)** XRD spectra of WSi and WAl and **e)** N_2 adsorption-desorption isotherms at 77 K and pore size distribution for WSi and WAl.

From the semi-quantitative chemical analysis (Figure 3a) and 3b)), WSi contains 38% by weight of Si and 35% of O, in addition ~~to~~ Na, Mg, Al, Ce are in proportions less than 10%. These last elements are part of the materials used in the polishing and finished glass process. WAl contains 43% Al, 33% O, and 13% Si. This residue comes from the grinding process, which is done using mainly aluminum oxide.

WSi and WAl FTIR spectra are shown in Figure 3c). The WSi spectrum shows the characteristic bands of the Si-O-Si bond at 1106 and 807 cm^{-1}. The peaks at 449 and 825 cm^{-1} are attributed to Si-O vibration, and the band at 1100 is assigned to Si-OH bonds. 1102 cm^{-1} corresponded to the stretching vibration of Si-O-Si. Peaks at 1977 cm^{-1} and 1875 cm^{-1} are overtones of Si-O vibrational modes and were seen in all spectra. The spectrum corresponding to WAl shows the characteristic bands of the Al_2O_3 links. The main peaks at 459, 595, and 656 cm^{-1} can be assigned to the Al–O stretching mode in the octahedral structure; bands around 715 cm^{-1} and 1072 cm^{-1} are related to Al–O stretching mode in a tetrahedron and symmetric bending of Al–O–H, respectively. The peak at 3500 cm^{-1} is attributed to the OH stretching vibration in WSi and WAl [40].

The amorphous state of the WSi material is observed in the XRD spectrum (Figure 3d), a diffuse band between 10° - 40° of 2θ assigned to the amorphous phase is identified. The WAl XRD spectrum shows peaks attributable to crystalline phases of Al_2O_3 (Figure 3d)). The textural properties of WSi and WAl show that the specific surface of WSi is more significant than that obtained for WAl (16.82 m^2 g^{-1} and 7.28 m^2 g^{-1}, respectively). The mean pore size for WSi is 23.40 nm, and the mean pore size for WAl is 26.50 nm (Figure 3e). It can be observed that both wastes have a small specific surface, but the pore diameter

for both wastes is characteristic of mesoporous materials (2 nm<Dp<50 nm) and comparable with synthesized materials [41, 42]. Also, the WSi and WAl wastes have a small pore volume of 0.181 cm^3 g^{-1} (micropore area is 0.876 m^2 g^{-1}) and 0.043 cm^3 g^{-1}, respectively.

3.2. CO_2 capture: Static system

The WSi and WAl wastes were exposed to a gas sample containing different concentrations of CO_2 in N_2 in a total volume of 25 mL. The CO_2 adsorption (%) curve and adsorption capacity (mmol CO_2 g^{-1}) were constructed simultaneously for different CO_2 concentrations (10-50% v/v of CO_2/N_2). CO_2 concentrations 10%, 16%, 24% and 50% v/v were selected, taking into account the existing percentages in the combustion gasses of different industrial activities such as coal power plants (12-14%), cement plants (14-33%) or coal gasification systems (30-35%) [43].

3.2.1. CO_2 adsorption capacities for WSi

Figure 4a) shows the effect of different carbon dioxide concentrations for WSi waste at 20°C and 1 atmosphere over the CO_2 adsorption (%).

The CO_2 adsorption (%) obtained for a concentration of 10% v/v CO_2/N_2 was 81.8%, and for the concentration of 16% v/v CO_2/N_2, an 82.2% adsorption of CO_2 was obtained. 250 mg of waste was used.

When the CO_2 concentration increases to 50%, the material absorbs 29.04% of the initial CO_2. It can be seen that as the amount of CO_2 increases, the percentage of CO_2 removal decreases. The effect of variation of CO_2 concentrations on the adsorption capacity of WSi residue (250 mg) was evaluated. Figure 4b) shows the CO_2 mmol adsorbed for different

CO_2 concentrations. As the CO_2 concentration increases, there is an increase in adsorption capacity for the same amount of solids adsorbents. For 16% and 50% v/v CO_2/N_2 concentrations, the WSi waste presented an adsorption capacity of 0.51 mmol CO_2 g^{-1} and 0.71 mmol g^{-1}, respectively.

Vittoni et al. (2019) [44], studied the capture capacity of a non-porous material based on silica (Stöber) comparing it with an MCM-41 silica material, resulting in a difference in the adsorption capacity of 15%. The silica-based sample (Stöber) has an adsorption capacity of 0.49 mmol g^{-1}. Compared with the silica-based residue (WSi) with an adsorption capacity of 0.51 mmol g^{-1} for CO_2/N_2 at 16/84% v/v, the WSi residue only differs with the porous material (MCM-41) by 12%.

Figure 4b) shows that the saturation of WSi waste occurs after 12 min of exposure in the different concentrations of CO_2/N_2. That is, CO_2 molecules have occupied most of the pores that the material had at that time. In turn, it can be observed that the adsorption rate is higher as the concentration of CO_2 increases in the gaseous sample.

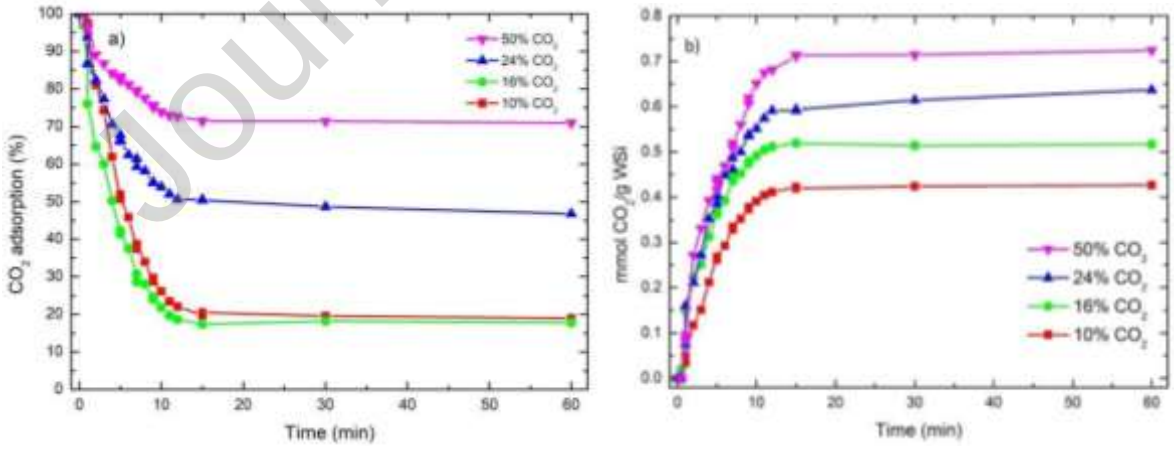

Figure 4. a) CO_2 adsorbed (%) over time and **b)** mmol of CO_2 adsorbed over time, for different concentrations of CO_2 and 250 mg of waste, WSi.

When the CO_2 concentration is below 0.84 mmol L^{-1} of CO_2 (18.9%), the physisorption process is no longer produced for 10% y 16% vol CO_2 in N_2 of the gas mixture concentration. It is observed that the adsorption capacity increases as the material is exposed to higher concentrations of CO_2. However, the C/Co ratio decreases for the same amount of waste WSi.

3.3.2. CO_2 adsorption capacities for WAl

A similar analysis was performed for WAl residue. The results were compared with the WSi residue. Figure 5a) shows the CO_2 adsorption (%) curves for different CO_2 concentrations 10%-50% v/v CO_2/N_2 over time. mmol of CO_2 adsorbed over time for different concentration of CO_2 is presented in Figure 5b).

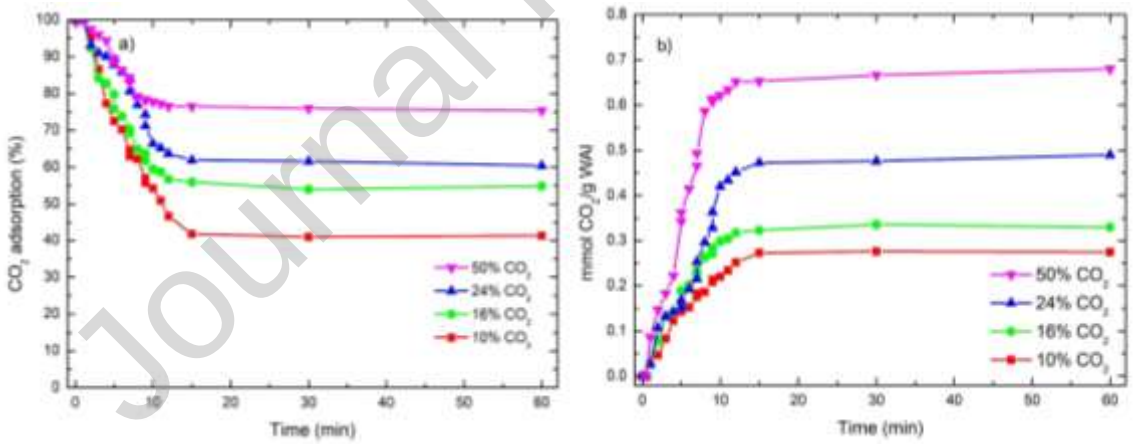

Figure 5. a) CO_2 adsorbed (%) over time and **b)** mmol of CO_2 adsorbed over time, for different concentrations of CO_2 and 250 mg of waste, WAl.

As a result, the C/Co ratio decreases for the same amount of WAl. Considering the initial concentration of CO_2 and the final concentrations, the efficiencies of the adsorption

processes were calculated. For 10 % initial CO_2 the removal efficiency is 61.0%, and the residual CO_2 is 1.74 mmol CO_2 L^{-1}. For 50%, the CO_2 removal efficiency is 27.2%, and the residual CO_2 is 17.48 mmol CO_2 L^{-1} (the residual CO_2 was calculated for a total time of 60 min).

The CO_2 adsorption capacities for different concentrations of CO_2 at 20°C and 1 atmosphere are presented in Figure 5b) in function of time. The adsorption capacity of 0.36 mmol CO_2 g^{-1} WAl waste for 10% v/v CO_2/N_2 and 0.68 mmol CO_2 g^{-1} for 50% v/v CO_2/N_2. This is due to the relationship between the maximum adsorption capacity and the availability of CO_2 in the gaseous sample at a given time. Figure 5b) shows that WAl waste is saturated after 14 min of exposure for the different concentrations of CO_2. The adsorption capacity (mmol g^{-1}) increases as the CO_2 concentration increases. It is observed that the adsorption values are getting more significant as the material is exposed to higher CO_2 concentrations.

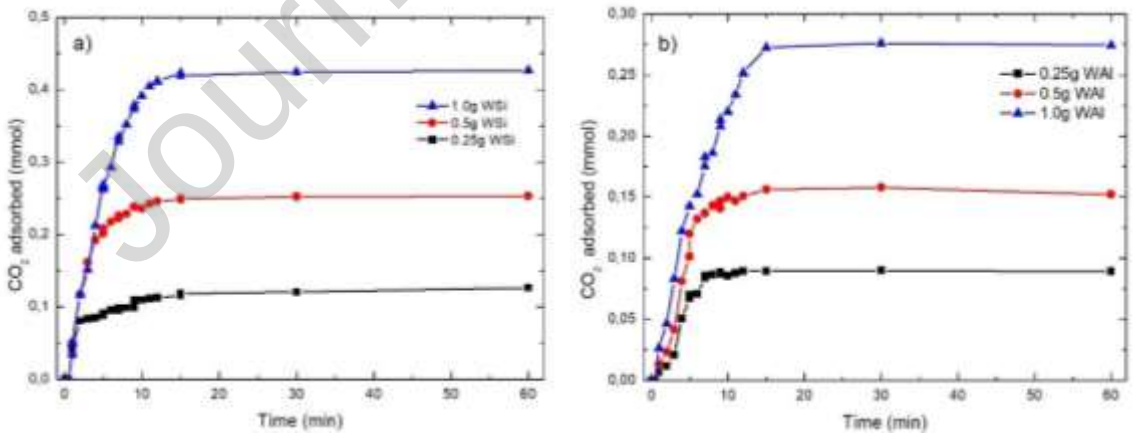

Figure 6. CO_2 adsorbed (mmol) over time for **a)** waste WSi for 10% CO_2 and **b)** waste WAl for 10% CO_2.

Comparing WSi and WAl, both residues behave in the same way, the adsorption curves have the same tendency. The adsorbed CO_2 (mmol) at 20°C and 1 atmosphere is presented in Figures 6a) and 6b) as a function of the amount of WSi and WAl wastes. As can be seen, the WSi has a higher CO_2 adsorption capacity than WAl for all the amounts studied. In all the experiments, as the amount of exposed solid increases, the adsorbed CO_2 increases in equal measure. The adsorption capacity of CO_2 in low concentrations (diluted streams 10% CO_2/N_2) was 80.5% for WSi and 61% for WAl after 60 minutes of interaction.

3.4. CO_2 capture: Dynamic system

Due to the importance of validate static results in a simulated real case, CO_2 capture was performed in a dynamic system by exposing the waste to different streams 330 and 660 mL min^{-1}. The final test time was 60 minutes.

Figure 7a) shows the adsorption capacity (mmol CO_2) per gram of WSi. Figure 7b) shows the relationship between the initial and final concentration at 60 min about the exposure time of WSi at different CO_2 concentrations. Due to the solid disposition, an S-shaped concentration profile is not observed, as is the one that can be found when the experiments are carried out in a fixed bed of solid. The waste is placed in the form of a bed, and the flow is circulated parallel to the surface. The curves are characterized by having two zones with partial adsorption and one zone with complete adsorption.

The WSi adsorption capacity values for 1 g of solid were 0.83 mmol for 10% CO_2, 0.97 mmol for 16 %CO_2, 1.23 mmol for 24 % CO_2, and 1.34 mmol for 50% CO_2. Chakravartula Srivatsa and Bhattacharya (2018) [45] evaluated the effect of the CO_2 concentration on the adsorption capacity in SBA-15 loaded with a different amine. The thermogravimetric study

showed that materials adsorption capacities increased with an increase in the concentration between 122% and 153% for 5% and 80% of CO_2 in the gas (flow 100 mL min^{-1}). A similar result was obtained in this work, showing an increase in adsorption capacity of 75% for 10% and 50% v/v CO_2/N_2 for 330 mL min^{-1}. In concentrations above 50% CO_2, no further adsorption occurs.

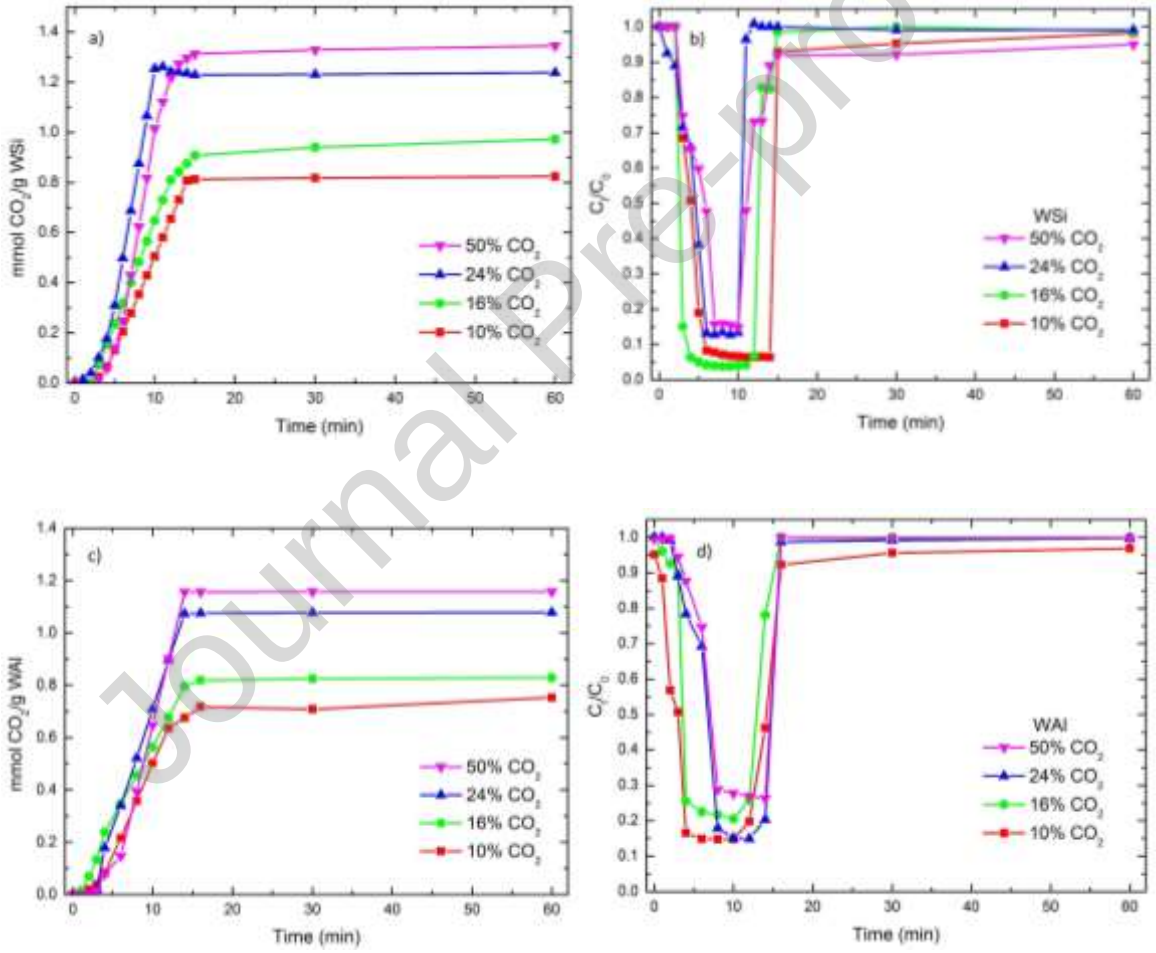

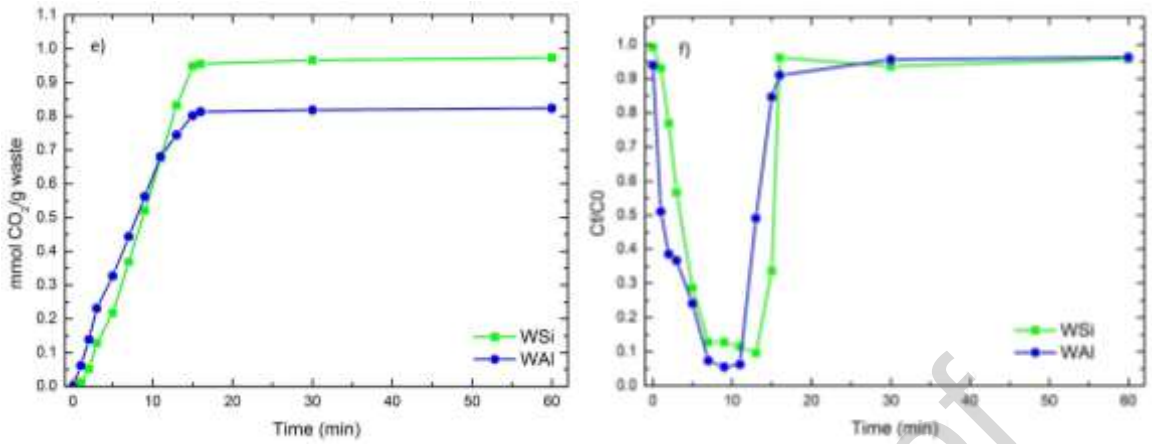

Figure 7. Evaluation of **a)** CO_2 adsorbed as a function of time for WSi, **b)** C_f/C_0 vs time with a flow rate of 330 mL min^{-1} for different concentration for WSi, **c)** CO_2 adsorbed as a function of time for WAl, **d)** C_f/C_0 vs time with a flow rate of 330 mL min^{-1} for different concentration for WAl, **e)** CO_2 adsorbed over time for WSi and WAl with a flow rate of 660 mL min^{-1} with 16% CO_2. **f)** C_f/C_0 vs time for WSi and WAl with a flow of 660 mL min^{-1} and 16% CO_2. Test temperature at 20°C.

Figure 7b) shows the adsorption curve about C_f/C_0 vs time for the WSi residue. The adsorption curves show well defined capture zones and partial capture or saturation zones with the solid exposure time to the gaseous stream. For gaseous mixtures of 10% of CO_2 in N_2, it can be seen that the maximum adsorption was between 91.00% and 93.62% during 6 minutes, and after 12 minutes, it was saturated. For 16% CO_2, adsorption occurs after 4 min with 89% capture, and after 12 min the material is saturated. Saturation of the material for 24% CO_2 and 50% CO_2 occurs after 10 minutes. However, for the flow composition of 50% CO_2, the adsorption process begins at 7 min reaching a maximum capture of 95%. Maximum adsorption of 88% for 24% CO_2 at 6 min was obtained.

Figure 7c) and 7d) shows the adsorption capacity (mmol CO_2) per gram of WAl and the relationship between the initial CO_2 concentration and after the adsorption test at 60 min, concerning the exposure time of WAl at different CO_2 concentrations. The adsorption capacity values for WAl were 0.75 mmol CO_2 g^{-1} for 10% CO_2, 0.83 mmol CO_2 g^{-1} for 16% CO_2, 1.07 mmol CO_2 g^{-1} for 24% CO_2 and 1.16 mmol CO_2 g^{-1} for 50% CO_2. In figure 7c), it is observed that at 6 minutes, the adsorption process begins (72%-74%), and saturation occurs at 12 minutes for 10% of CO_2 in N_2. Saturation of WAl for 16% and 24% of CO_2 occurs at 14 minutes, and the adsorption process begins at 4 min for both.

Figure 7e) shows the adsorption capacity of WSi and WAl as a function of time for a gas flow of 660 mL min^{-1}, twice that used in the previous tests. It was observed that a higher gas flow produces saturation of the wastes at shorter times and accelerates the CO_2 capture that appears at the beginning of the test. At 10 min elapsed of the capture test, WSi adsorbed 0.647 mmol CO_2 g^{-1} and 0.680 mmol CO_2 g^{-1} for a flow of 330 mL min^{-1} and 660 mL min^{-1}, respectively. For WAl, a similar behavior occurs at 10 min; the capacity is 0.566 mmol CO_2 g^{-1} and 0.744 mmol CO_2 g^{-1} for 330 mL min^{-1} and 660 mL min^{-1}, respectively. For WSi and WAl, capacity values of 0.973 and 0.823 mmol CO_2 g^{-1} solid were obtained, respectively. These values are similar to those obtained in previous tests with a flow of 330 mL min^{-1}. The increase in CO_2 concentrations (in N_2) produces an increase in the values of CO_2 removal capacities and the CO_2 adsorption rate; that is, the adsorption process is kinetically favored.

The values of mmol CO_2 per gram of material for both flows studied (660 mL min^{-1} and 330 mL min^{-1}) are similar (Fig. 7f)). However, it was observed that for both materials, saturation occurs after 15 min, and the maximum adsorption zone for WSi is between 6 and

14 minutes. For WAl it is between 6 and 12 min, this adsorption period being responsible for the differences obtained in the maximum capture capacity. As the gas flow increases, it causes a decrease in the saturation time. The slope in the adsorption stage is more pronounced, suggesting that the transfer speed of external matter influences the rate of the adsorption process. An increase in operating flows improves the adsorption process generating higher rates of CO_2 adsorption for both wastes. The comparison between adsorption capacities in static and dynamic systems for the wastes exposed to different CO_2 concentrations is shown in Table 2.

In both systems, as the CO_2 concentration in the gas mixture (CO_2/N_2) increases, an increase in adsorption capacity can be observed, but the residual CO_2 is higher. This behavior is precisely due to the nature and the capacity of the material. The dynamic system has a difference in the value of residual CO_2 for concentrations of 24% CO_2/N_2 because the adsorption, in this case, reaches percentages less than 90%, showing higher residual values.

Table 2. The adsorption capacity for WSi and WAl exposed to different CO_2 concentrations in static and dynamic systems (flow 330 mL min^{-1}).

System	Concentration (%v/v)	WSi (mmol/g adsorbent)	Residual CO_2 (%)	WAl (mmol/g adsorbent)	Residual CO_2 (%)
Static (25 mL)	10% CO_2	0.43	19.66	0.27	39.00
	16% CO_2	0.51	27.18	0.33	49.55
	24% CO_2	0.63	40.53	0.49	54.29
	50% CO_2	0.72	72.78	0.68	78.21
Dynamic (330 mL min^{-1})	10% CO_2	0.83	84.27	0.75	93.6
	16% CO_2	0.97	98.25	0.83	98.9
	24% CO_2	1.23	99.12	1.07	99.2
	50% CO2	1.34	99.31	1.16	99.4

The amount of residual CO_2 (%) was calculated for the maximum adsorption obtained in a given time (60 min).

Tiwari et al. (2017) [46], studied the adsorption capacity of carbon adsorbent materials prepared using mesoporous zeolite and melamine-formaldehyde resin. They evaluated the CO_2 adsorption at different temperatures (30-100ºC) and concentrations (5-12.5%) in a dynamic column with a fixed bed. It can be observed that as the concentration of CO_2 increases there is an increase in the adsorption capacity of the materials. The best adsorbent showed 0.64 mmol CO_2 g^{-1} at 30°C with 12.5% of CO_2 initial concentration. By increasing the initial concentration of CO_2 by 5%, they obtained an increase of 0.21 mmol CO_2 g^{-1} of material. Comparing the values obtained in this work, it can be observed that at 20ºC and with an increase of CO_2 of 5% in the gas flow, there is an increase in the adsorption capacity of 0.15 mmolCO_2 g^{-1} WSi.

3.4.1. Effect of temperature on capture test

In a real scenario, the combustion gases vary both in composition and in conditions. Therefore, to evaluate the performance of materials it is necessary to test the absorption capacity at different temperatures. The effect of the increase in temperature on the adsorption capacity of the WSi residue was evaluated, which showed in the previous tests greater efficiency in CO_2 capture. Figure 8a) shows that as the temperature increases, there is a decrease in the mmol of CO_2 adsorbed per gram of WSi. For a temperature of 20°C a value of 0.972 mmol CO_2 g^{-1} WSi was obtained.

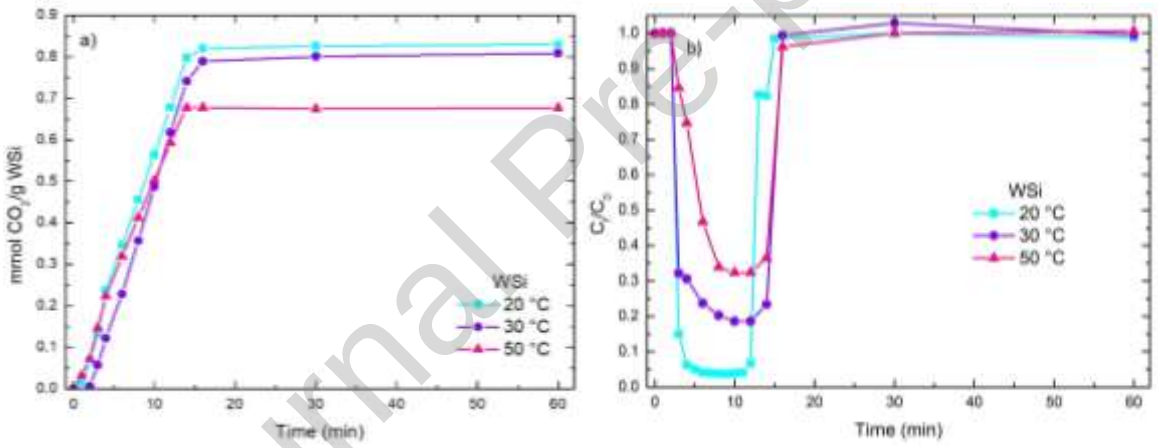

Figure 8. Evaluation of different temperatures: **a)** mmol of adsorbed CO_2 as a function of time for WSi, **b)** variation of concentration as a function of time, with a flow of 330 mL min^{-1} to 16% v/v of CO_2/N_2.

Saturation time is 15 min with a 94% reduction in the CO_2 concentration. At temperatures of 30°C and 50°C, values of 0.808 mmol CO_2 g^{-1} WSi and 0.676 mmol CO_2 g^{-1} WSi were obtained. In Figure 8b) the variation of CO_2 concentration as a function of time is shown. The initial CO_2 concentration decreased by 86% and 69% for 30°C and 50°C respectively.

The use of high flows and an increase in operating temperature can improve the mobility of the molecules adsorbed on the surface of WSi, which would cause a decrease in the adsorption capacity of CO_2 due to the forced migration of the molecules (physisorption process). Singh and Kumar (2016) [42], measured the adsorption and kinetic isotherms of CO_2 on activated carbon and zeolite 5A samples at different temperatures (298, 308, 318, and 338K) and pressures (1, 5, 10 and 20 bar). These authors observed that as the temperature increases, the adsorption capacity decreases. For a pressure of 1 bar, an increase in temperature from 298K to 308K (3%) causes a 9% decrease in the adsorption capacity.

Regarding the adsorption times, it can be observed that the material is saturated above 13-15 minutes and no longer adsorbs CO_2. This same behavior is observed in static tests.

Figure 8a) shows the CO_2 adsorption kinetics in the WSi waste for different temperatures, at atmospheric pressure and 16% vol CO_2. To evaluate the effect of temperature on the CO_2 adsorption kinetics in WSi, the experimental values obtained were modeled using a pseudo-first order (2), pseudo-second order (3) and Avrami equation (4).

As shown in Table 3, the parameters predicted by the models, such as adsorption rate constants, increase with temperature for the pseudo-first order model. However, in the pseudo-second order and Avrami models, the opposite occurs.

Table 3. Parameters of the pseudo-first order, pseudo-second order and Avrami models for the adsorption of CO_2 in WSI for 20°C, 30°C and 50ºC, 16% vol CO_2.

	Pseudo-first order			Pseudo-second order			Avrami model			
Temperature (°C)	q_e (mmol/g)	k_f (1/min)	R^2	q_e (mmol/g)	k_s (mmol/gmin)	R^2	q_e (mmol/g)	k_A	n_A	R^2
20	0.965	0.115	0.986	0.965	0.293	0.983	0.881	0.117	1.743	0.974
30	0.857	0.111	0.981	0.921	0.291	0.984	0.786	0.097	1.953	0.957
50	0.671	0.107	0.987	0.760	0.240	0.988	0.582	0.066	1.478	0.945

The pseudo-first order is the model that has the closest values to those obtained experimentally with the CO_2 adsorption capacities at 20°C, 30°C and 50°C, with correlation coefficients (R^2>0.98). Comparing the values of the experimental CO_2 adsorption capacity and q_e obtained by the models, a considerable difference is observed when a pseudo-second order model is applied. In other words, the model has a greater dispersion at high exposure times, so it is not considered a model that fits well with the experimental data obtained.

Thus, the pseudo-second order and Avrami do not accurately model the experimental data of CO_2 adsorption at different temperatures. Adsorption is improved at low temperature, so increasing the adsorption temperature causes a decrease in the rate constant k_f. The pseudo-first order kinetic model can predict the physisorption of CO_2 in this material as in oxides and carbons.

Sravanthi Loganathan et al. (2014) [47] studied the CO_2 adsorption kinetics on mesoporous silica under certain pressure (0.2-1.1 bar) and temperature (30, 45, 60 and 75°C) ranges. The experimental results of CO_2 capture as a function of time were analyzed with pseudo-first order and pseudo-second order kinetic models. The kinetic model of pseudo-first order successfully writes the adsorption kinetics of CO_2 on silica in the entire range of pressure and temperature regime, suggesting that the adsorption process in this type of materials is controlled by physisorption. Accordingly with this work, the kinetic model that best fits the experimental results is the pseudo-first order.

3.5. WSi and WAl reuse cycles

The regeneration of these adsorbents is essential when assessing their application on an industrial scale. Figure 9 shows the adsorption capacity of WSi and WAl for a concentration of 10% CO_2 and at temperature *ca.* 20°C. It was evaluated for a time of 60 min for both samples. In addition, the removal of adsorbed CO_2, described in section 2.3, was carried out between each test. It can be observed in Figure 9 that the adsorption capacity decreased from 0.427 to 0.397 mmol g^{-1} for WSi. In contrast, the adsorption capacity for WAl decreased from 0.274 to 0.266 mmol g^{-1}, after the first cycle of regeneration operation. After 5 cycles, the capacities decrease by 7%, for WSi and 3% for WAl, suggesting that most CO_2 molecules can be effectively physically desorbed from the residue surface at 100°C for 60 min.

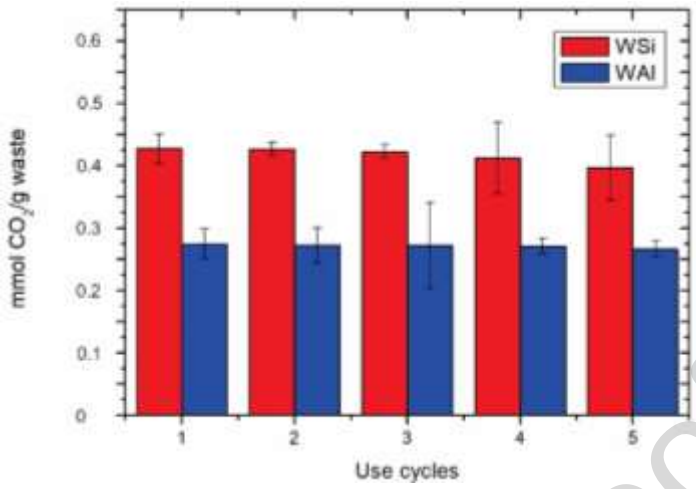

Figure 9. Reuse cycles for CO_2 adsorption in waste WSi and WAl.

These results show that the wastes have a high reuse capacity in consecutive CO_2 capture systems and can regenerate through an increase in temperature and an N_2 stream.

3.6. Capture tests on real samples

One of the objectives of using waste in the adsorption of CO_2 is the importance of eliminating the energy and environmental costs of synthesis and that they are applicable in real gaseous streams or post-combustion of different companies or industries that emit this gas. In the first sections, the study was carried out in this work on simulated samples. Still, in this section, the efficiency of the waste in different gaseous effluents is evaluated. Combustion gases from carbonization processes contain high percentages of CO_2 and water. In this work, the capacities to capture CO_2 from real combustion gases of WSi and WAl wastes were evaluated. The real samples were taken at the exit of a charcoal-making furnace. The raw material for the production of coals were residues from a local flour mill and residues from a local brewing industry. The flue gases samples were taken at 500°C.

The capture test was conducted for an exposure time of 20 min and a final volume of 25 mL.

For the adsorption evaluation, FTIR was used. The areas of the characteristic bands of the different compounds present in gasses samples were measured to obtain the efficiency of WSi and WAl at different exposure times. For CO_2 the area under the curve of the three characteristic regions was measured 726.97 cm^{-1}-580.47 cm^{-1}, 2414 cm^{-1}- 2198 cm^{-1} and 3662.20 cm^{-1}- 3752.84 cm^{-1}. The two distinct regions evaluated for the presence of H_2O are 1712.5 cm^{-1}-1402.01 cm^{-1} and 3936.05 cm^{-1}- 3774.06 cm^{-1}. In turn, the water content was measured according to the exposure time.

Figure 10a) shows the areas calculated for different exposure times to gas from the carbonization of beer residue. It can be seen that the water content and the CO_2 content decrease as the capture time increases. It can be seen that the WSi waste produces a reduction of the CO_2 content of the stream by 49.8% and the WAl waste by 38.1%. The water content decreases by 26.2% when WSi is used and by 25.3% for WAl. The water content in flour mill waste flue gases is higher than in the gases of the beer waste.

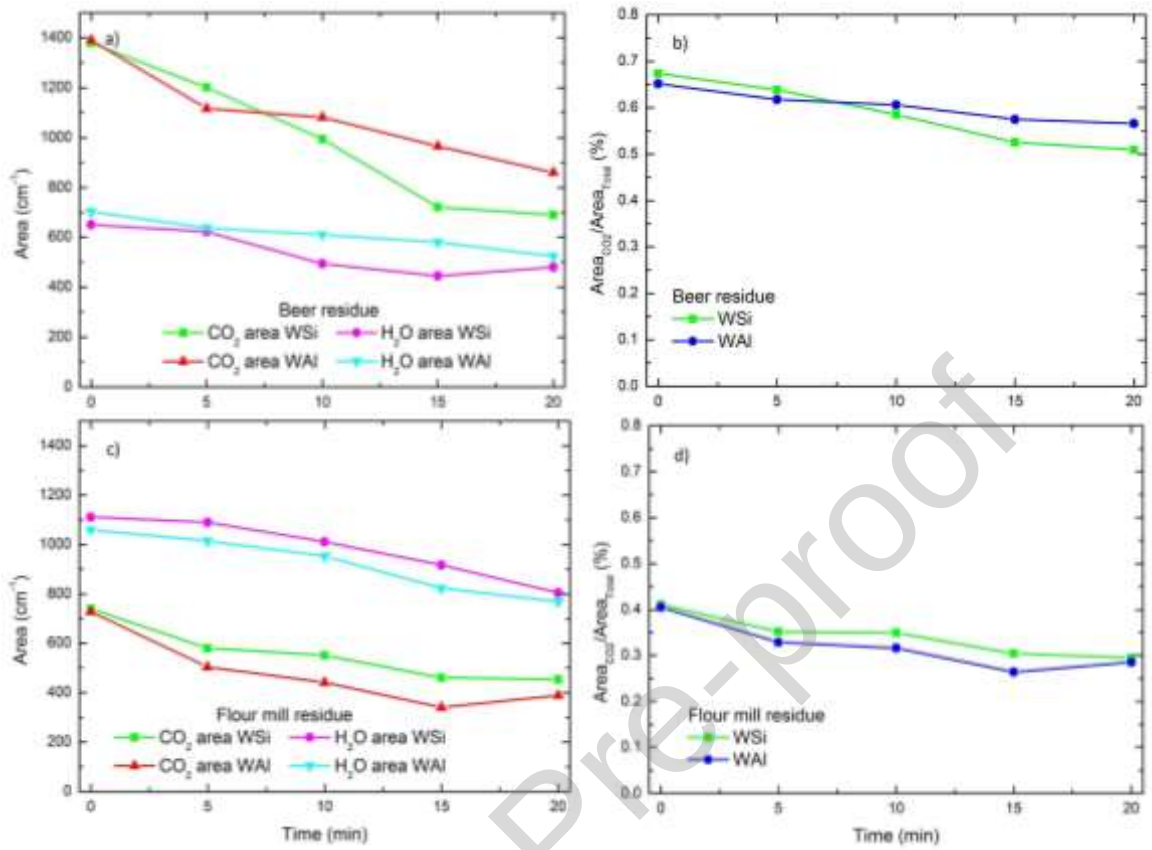

Figure 10. Capture test of real gaseous samples by carbonization of beer waste **a)** Area under the curve vs exposure time for WSi and WAl adsorption test, **b)** $Area_{CO2}/Area_{total}$ (%) vs exposure time. Capture test of real gaseous samples by flour mill waste, **c)** Area under the curve vs exposure time for WSi and WAl adsorption test, **d)** $Area_{CO2}/Area_{total}$ (%) vs exposure time.

Figure 10c) shows the area calculated through FTIR spectra as a function of the exposure time to real gaseous samples from the calcination of flour mill waste.

The CO_2 content is reduced by 46% when WAl is used and by 38% for WSi. The reduction of water content is 27.5% in coincidence for the WSi and WAl residues. In this case, the capture values are smaller than those obtained with the beer combustion gases; this

difference may be due to the presence of water in greater proportions [48]. Comparing Figure 10a) and Figure 10c), the CO_2 content is higher in the flue gases when the beer production waste is charred, approximately double by comparing the area under the curve.

The combustion gases of the beer waste contain an $Area_{CO2}/Area_{total}$ of 65%, whereas in the combustion gases of the flour mill waste, the CO_2 content is $Area_{CO2}/Area_{total}$ of 40% (Figure 10b) and Figure 10d)). If we compare the reduction about the fraction of CO_2, it can be seen in Figure 10 b) a reduction of CO_2 of 16% in 20 min under environmental conditions for WSi and of 8% for WAl. Figure 10 d) shows a decrease in $Area_{CO2}/Area_{total}$ for WSi of 13% and for WAl of 12%. In this case, similar behaviour of WSi and WAl waste is observed, which shows that the presence of H_2O in gaseous streams is one of the causes of the decrease adsorption efficiency on materials of this nature.

The application of the residual materials WSi and WAl showed a good performance in CO_2 capture and adsorption kinetics. A study was carried out in a static and another one in a dynamic bed system on a laboratory scale with CO_2/N_2 simulated multicomponent samples in different concentrations, and the reuse cycles were evaluated by applying a high temperature desorption stage. These adsorbent materials were tested in turn in real samples of combustion gases where the effect of competition on the adsorption of H_2O and CO_2 could be observed. However, when the main goal is to apply these residual materials in large-scale systems, obtaining a good adsorbent material is not the only thing to consider. The configurations of the adsorption reactors (depending on the particle size and the solid-gas contact) and the regeneration mode of the materials are crucial to designing efficient and low-cost adsorption processes. Also, to determine whether or not these wastes can be applied on a large scale, we must take into account the granular characteristics of the

material, which are fine powders and it would be best to use a fluidized bed to avoid agglomeration and the formation of channels [12, 49]. Regarding the regeneration modes, using other modes it is possible to have a higher performance in the successive uses of the materials.

According to Raganati et al. (2021), the commercial post-combustion CO_2 capture systems show a slow development due to the significant cost of the capture phase, which represents approximately 2/3 of the total cost of CCS. There are limited studies on techno-economic evaluation of adsorption-based CO_2 capture, and those presented are not systematic enough to provide conclusions about the best adsorbent material/reactor type/regeneration mode combinations [6].

On the other hand, many adsorbent materials and their synthesis techniques show a considerable disparity in cost analysis. According to Tarka et al., in 2006, a competitive sorbent cost should be 5$/kg [50] and actualized in 2020 for Abd et al., the cost should be around 10$/kg [13]. Although the objective of this work is not to analyze the cost of the proposed system, it should be noted that there are no synthesis costs (economic and environmental) since industrial waste is used as sorbent. In addition, there is a reduction in environmental and economic costs associated with the final non-disposal of waste for the glass industry that generates it. In terms of configuration and regeneration mode, according to Dhoke et al. (2021), the highest cost is associated with the regeneration of the material (TSA) due to the energy consumption in the desorption stage. However, the proposed capture system is based on a physisorption process where the temperature required is not as high as in a chemisorption process, which considerably reduces the energy cost [5].

Conclusions

In this work, two wastes from the glass processing industry were used to adsorb CO_2 from real and simulated gas streams. The residues were ~~only~~ dried at 90 °C and mechanically ground before use. This promotes a reduction in energy and the environmental cost concerning other oxides synthesized in the laboratory. The characterization showed that they contain silica and alumina in their composition and other metals from the products used in each industrial process. A non-porous morphology is evidenced in both but with plate-like particles. The residue that contains silica as the most significant component is amorphous, while the one that contains alumina presents its characteristic peaks. The WSi showed the best performance in capturing CO_2, even at different working temperatures for the static and dynamic system.

The good agreement between the results of the pseudo-first-order kinetic model and the experimental data shows that the kinetic constants obtained from this work are appropriate for the design of capture processes. The maximum adsorption capacities coincide with the highest specific surface product, so, the most efficient is WSi residue. It was possible to evaluate CO_2 reduction and adsorption performance when H_2O and other compounds are present by exposing the waste with actual samples of flue gases generated by the carbonization of biomass waste. Reducing environmental pollution through the reuse and recovery of waste is essential for protecting present and future generations, so these results encourage future capture applications and provide a technological solution for the disposal of the abundant glass industry residue.

Summarizing, in the present work, the use of industrial waste to capture CO_2 is presented. These contain alumina and silica because they are waste in the glass polishing and finishing processes. Through their physicochemical characterization and the evaluation of their adsorption capacity, it was determined that they could be used to capture CO_2 with yields comparable to those obtained by other researchers with these oxides synthesized in the laboratory. Thus, through this study, the alternative of using this type of waste to capture CO_2 is proposed with a considerable reduction in energy and environmental cost caused by synthesis methods. They were also found to be optimal for use in actual gas streams generated in different industries.

Acknowledgements

The authors thank Lic. Lucas dos Santos for helping in the preparation of the characterization of the waste WSi and WAl. The industry for the contribution of waste for this project. Eng. Maria Beatriz Silverii for his help in the capture test and FTIR. Marcelo Federico Ponce is a doctoral fellowship holder of the CONICET. Florencia Jerez is a doctoral fellowship holder of the CONICET. Gaston Pablo Barreto is a researcher of CONICET. Marcela Alejandra Bavio is a researcher of CONICET.

Funding

This study was supported by the Engineering Faculty, Secretary of Science, Art and Technology of the National University of the Center of the Province of Buenos Aires, Project 03/E188 and the National Agency for Scientific and Technological Promotion (ANPCyT) through the Fund for Scientific and Technological Research (FONCyT), Project PICT2019-03745, and Project PUE 2017.

References

[1] Intergovernmental Panel on Climate Change. (2015). Climate Change 2014: Mitigation of Climate Change: Working Group III Contribution to the IPCC Fifth Assessment Report. Cambridge: Cambridge University Press. https://doi.org/10.1017/CBO9781107415416.

[2] WMO GREENHOUSE GAS BULLETIN, The State of Greenhouse Gases in the Atmosphere Based on Global Observations through 2017. Nro. 14, 22/11/2018.

[3] Banco Mundial, access 2019. https://www.bancomundial.org

[4] SGAyDS. 2019. Tercer Informe Bienal de Actualización de Argentina a la Convención Marco de las Naciones Unidas para el Cambio Climático (CMNUCC).

[5] C. Dhoke, A. Zaabout, S. Cloete, and S. Amini. 2021. Review on Reactor Configurations for Adsorption-Based CO_2 Capture. Industrial Engineering Chemistry Research, 60, 3779−3798. https://dx.doi.org/10.1021/acs.iecr.0c04547

[6] F. Raganati, F. Miccio, and P. Ammendola. 2021. Adsorption of Carbon Dioxide for Post-combustion Capture: A Review. Energy Fuels 35 (16) 12845–12868. https://doi.org/10.1021/acs.energyfuels.1c01618

[7] C. Dhoke, S. Cloete, S. Krishnamurthy, H.S.I. Luz, M. Soukri, Y. Park, R. Blom, S. Amini, A. Zaabout. 2020. Sorbents screening for post-combustion CO_2 capture via combined temperature and pressure swing adsorption. Chemical Engineering Journal 380, 122201. https://doi.org/10.1016/j.cej.2019.122201

[8] P. Ammendola, F. Raganati, R. Chirone, F. Miccio. 2020. Fixed bed adsorption as affected by thermodynamics and kinetics: Yellow tuff for CO_2 capture. Powder Technology 373, 446–458. https://doi.org/10.1016/j.powtec.2020.06.075

[9] M.D. D'Alessandro, B. Smit, J.R. Long. 2010. Carbon Dioxide Capture: Prospects for New Materials Angew. Chem. Int. Ed. 49, 6058 – 6082. https://doi.org/10.1002/anie.201000431

[10] T.H. Pham, B.K. Lee, J. Kim, C.H. Lee. 2016. Enhancement of CO_2 capture by using synthesized nano-zeolite. Journal of the Taiwan Institute of Chemical Engineers. 64, 220-226. https://doi.org/10.1016/j.jtice.2016.04.026.

[11] Y. Liu, J. Hu, X. Ma, J. Liu, Y.S. Lin. 2016. Mechanism of CO_2 adsorption on Mg/DOBDC with elevated CO_2 loading. Fuel. 181, 340-346. https://doi.org/10.1016/j.fuel.2016.04.142

[12] F. Raganati and P. Ammendola. 2021. Sound-Assisted Fluidization for Temperature Swing Adsorption and Calcium Looping: A Review. Materials 14, 672. https:// doi.org/10.3390/ma14030672

[13] A.A. Abd, S.Z. Naji, A.S. Hashim, M.R. Othman. 2020. Carbon dioxide removal through physical adsorption using carbonaceous and non-carbonaceous adsorbents: A review. Journal of Environmental Chemical Engineering 8, 104142. https://doi.org/10.1016/j.jece.2020.104142.

[14] Y. Boyjoo, Y.Cheng, H. Zhong, H. Tian, J. Pan, V.K. Pareek, V.K., S. Ping Jiang, J. Lamonier, M. Jaroniec, J. Liu. 2017. From waste Coca Cola® to activated carbons with impressive capabilities for CO_2 adsorption and supercapacitors. Carbon 116, 490-499. https://doi.org/10.1016/j.carbon.2017.02.030

[15] A.D. Igalavithana, S.W. Choi, P.D. Dissanayake, J. Shang, C-H. Wang, X. Yang, S. Kim, D.C.W. Tsang, K.B. Lee, Y.S. Ok. 2020. Gasification biochar from biowaste (food waste and wood waste) for effective CO_2 adsorption. Journal of Hazardous Materials 391, 121147. https://doi.org/10.1016/j.jhazmat.2019.121147

[16] A. Nawar, H. Ghaedi, M. Ali, M. Zhao, N. Iqbal, R. Khan. 2019. Recycling waste-derived marble powder for CO_2 capture. Process Safety and Environmental Protection 132, 214-225. https://doi.org/10.1016/j.psep.2019.10.005

[17] M.A. Hernandez, A. Pestryakov, R. Portillo, M.A. Salgado, F. Rojas, E. Rubio, S. Ruiz, V. Petranovskii. 2015. CO_2 Sequestration by Natural Zeolite for Greenhouse Effect Control. Procedia Chemistry 15, 33-41. https://doi.org/10.1016/j.proche.2015.10.006

[18] S. Kumar, R. Srivastava, J. Koh. 2020. Utilization of zeolites as CO_2 capturing agents: Advances and future perspectives. Journal of CO_2 Utilization, 41, 101251. https://doi.org/10.1016/j.jcou.2020.101251

[19] M. Boscherini, F. Miccio, E. Papa, V. Medri, E. Landi, F. Doghieri, M. Minelli. 2020. The relevance of thermal effects during CO_2 adsorption and regeneration in a geopolymer-zeolite composite: experimental and modelling insights. Chemical Engineering Journal. 408, 127315. https://doi.org/10.1016/j.cej.2020.127315

[20] M. Younas, M. Rezakazemi, M. Daud, M.B. Wazir, S. Ahmad, N. Ullah, S. Inamuddin, Ramakrishna. 2020. Recent progress and remaining challenges in post-combustion CO_2 capture using metal-organic frameworks (MOFs). Progress in Energy and Combustion Science, 80, 100849. https://doi.org/10.1016/j.pecs.2020.100849.m

[21] J.L.C. Rowsell, O.M. Yaghi. 2004. Metal–organic frameworks: a new class of porous materials. Microporous and Mesoporous Materials. 73, 3–14. https://doi.org/10.1016/j.micromeso.2004.03.034

[22] F. Wang, C. Gunathilake, M. Jaroniec. 2016. Development of mesoporous magnesium oxide–alumina composites for CO_2 capture. Journal of CO_2 Utilization. 13, 114–118. https://doi.org/10.1016/j.jcou.2015.11.001

[23] W.M. Picanço, B.A. Feitosa, N.G. Da Silva, G.T.A. Silva, V.M. Giacon, P.H. Campelo, S.M. de Souza, K.M.T de Oliveira, E.A. Sanches, E.A. 2018. Aniline-oriented polymerization over nano-SiO_2 particles. Journal of Molecular Structure. 1167, 118-126. https://doi.org/10.1016/j.molstruc.2018.04.087

[24] F. Su, C. Lu, S. Kuo, W. Zeng. 2010. Adsorption of CO_2 on Amine-Functionalized Y-Type Zeolites. Energy Fuels. 24, 1441–1448. https://doi.org/10.1021/ef901077k

[25] G.T. Rochelle. 2009. Amine Scrubbing for CO_2 Capture. Science. 325, 1652–1654. https://doi.org/10.1126/science.1176731

[26] M. Asif, M. Suleman, I. Haq, S.A Jamal. 2018. Post-combustion CO_2 capture with chemical absorption and hybrid system: Current status and challenges. Greenhouse Gases: Science and Technology. 1-9. https://doi.org/10.1002/ghg.1823

[27] R. Idem, M. Wilson, P. Tontiwachwuthikul, A. Chakma, A. Veawab, A. Aroonwilas, D. Gelowitz. 2006. Pilot Plant Studies of the CO_2 Capture Performance of Aqueous MEA and Mixed MEA/MDEA Solvents at the University of Regina CO_2 Capture Technology Development Plant and the Boundary Dam CO_2 Capture Demonstration Plant. Ind. Eng. Chem. Res. 45, 8, 2414–2420. https://doi.org/10.1021/ie050569e

[28] S. Moioli, L.A. Pellegrini, M.T. Ho, D.E. Wiley. A comparison between amino acid based solvent and traditional amine solvent processes for CO_2 removal. 2019. Chem. Eng. Res. and Des. 46, 509–517. https://doi.org/10.1016/j.cherd.2019.04.035

[29] F. Tzirakis, I. Tsivintzelis, A. I. Papadopoulos, P. Seferlis. Experimental investigation of phase change amine solutions used in CO_2 capture applications: Systems with dimethylcyclohexylamine (DMCA) and N–cyclohexyl-1,3-propanediamine (CHAP) or 3-methylaminopropylamine (MAPA). 2021. Int. J. of Greenh. Gas. Control. 109, 103353.

[30] J. Park, N.F. Attia, M. Jung, M.E. Lee, K. Lee, J. Chung, H. Oh. 2018. Sustainable nanoporous carbon for CO_2, CH_4, N_2, H_2 adsorption and CO_2/CH_4 and CO_2/N_2 separation. Energy. 158, 9-16. https://doi.org/10.1016/j.energy.2018.06.010

[31] Y.G. Ko, S.S. Shin, U.S. Choi. 2011. Primary, secondary, and tertiary amines for CO_2 capture: Designing for mesoporous CO_2 adsorbents. Journal of Colloid and Interface Science. 361, 594–602. https://doi.org/10.1016/j.jcis.2011.03.045

[32] W. Chaikittisilp, H.J. Kim, C.W. Jones. 2011. Mesoporous Alumina-Supported Amines as Potential Steam-Stable Adsorbents for Capturing CO_2 from Simulated Flue Gas and Ambient Air, Energy Fuels. 25, 5528-5537. https://doi.org/10.1021/ef201224v

[33] A. Popa, S. Borcanescu, I. Holclajtner-Antunović, D. Bajuk-Bogdanović, S. Uskoković-Marković. 2021. Preparation and characterisation of amino-functionalized pore-expanded mesoporous silica for carbon dioxide capture. Journal of Porous Materials 28, 143–156. https://doi.org/10.1007/s10934-020-00974-1

[34] E.S. Sanz-Pérez, M. Olivares-Marín, A. Arencibia, R. Sanz, G. Calleja, M.M. Maroto-Valer. 2013. CO_2 adsorption performance of amino-functionalized SBA-15 under post-combustion conditions. Int. J. Greenhouse Gas Control. 17, 366-375. https://doi.org/10.1016/j.ijggc.2013.05.011

[35] E.S. Sanz-Pérez, T.C.M. Dantas, A. Arencibia, G. Calleja, A.P.M.A. Guedes, A.S. Araujo, R. Sanz. 2017. Reuse and recycling of amine-functionalized silica materials for CO_2 adsorption. Chemical Engineering Journal. 308, 1021-1033. https://doi.org/10.1016/j.cej.2016.09.109

[36] M. Ojeda, M. Mazaj, S. Garcia, J. Xuan, M.M. Maroto-Valera, N. Zabukovec Logar. 2017. Novel amine-impregnated mesostructured silica materials for CO_2 capture. Energy Procedia. 114, 2252-2258. https://doi.org/10.1016/j.egypro.2017.03.1362.

[37] G. Gómez-Pozuelo, E.S. Sanz-Pérez, A. Arencibia P. Pizarro, R. Sanz, D.P. Serrano. 2019. CO_2 adsorption on amine-functionalized clays. Microporous and Mesoporous Materials 282 (2019) 38-47.

[38] P. Qiuyun, W. Yi, W. Xiaocheng, S. Zhitao, W. Shikun, W. Junya, N. Ping, L. Shijian, H. Liang, W. Qiang. 2021. Biomass-derived carbon/MgO-Al_2O_3 composite with superior dynamic CO_2 uptake for post-combustion capture application. Journal of CO_2 Utilization 54, 101756.

[39] S.N. Kudahia, A.R. Noorpoor, N.M. Mahmoodi. 2017. Determination and analysis of CO_2 capture kinetics and mechanisms on the novel graphene-based adsorbents. Journal of CO_2 Utilization. 21, 17-29. https://doi.org/10.1016/J.JCOU.2017.06.010

[40] K. Djebaili, Z. Mekhalif, A. Boumaza, A. Djelloul. 2015. XPS, FTIR, EDX, and XRD Analysis of Al_2O_3 Scales Grown on PM2000 Alloy. K. Journal of Spectroscopy (2015) 1-16. https://doi.org/10.1155/2015/868109

[41] F. Wang, C. Gunathilake, M. Jaroniec. 2016. Development of mesoporous magnesium oxide–alumina composites for CO_2 capture. Journal of CO_2 Utilization. 13, 114–118. https://doi.org/10.1016/j.jcou.2015.11.001

[42] V.K. Singh and E.A. Kumar. 2016. Comparative Studies on CO_2 Adsorption Kinetics by Solid Adsorbents Energy Procedia. 90, 316 – 325. https://doi.org/10.1016/j.egypro.2016.11.199

[43] C-C. Cormos, F. Starr, E. Tzimas, S. Peteves. 2008. Innovative concepts for hydrogen production processes based on coal gasification with CO_2 capture. International Journal of Hydrogen Energy. 33, 1286-1294. https://doi.org/10.1016/j.ijhydene.2007.12.048

[44] C. Vittoni, G. Gatti, G. Paul, F. Mangano, S. Brandani, C. Bisio, L. Marchese. 2019. Non- Porous versus Mesoporous Siliceous Materials for CO_2 Capture. ChemistryOpen. 8 (6), 719-727. https://doi.org/10.1002/open.201900084

[45] Chakravartula Srivatsa, S., Bhattacharya, S. 2018. Amine-based CO_2 capture sorbents: A potential CO_2 hydrogenation catalyst. Journal of CO2 Utilization. 26, 397-407

[46] D. Tiwari, C. Goel, H. Bhunia, P.K. Bajpai. 2017. Dynamic CO_2 capture by carbon adsorbents: Kinetics, isotherm and thermodynamic studies Separation and Purification Technology. 181, 107–122. https://doi.org/10.1016/j.seppur.2017.03.014

[47] S. Loganathan, M. Tikmani, S. Edubilli, A. Mishra, A.K. Ghoshal. 2014. CO_2 adsorption kinetics on mesoporous silica under wide range of pressure and temperature. Chemical Engineering Journal. 256, 1–8. http://dx.doi.org/10.1016/j.cej.2014.06.091

[48] G. Li, P. Xiao, P.A. Webley, J. Zhang, R. Singh. 2009. Competition of CO_2/H_2O in Adsorption Based CO_2 Capture. Energy Procedia. 1, 1123–1130. https://doi.org/10.1016/j. egypro.2009.01.148

[49] J. Pirklbauer, G. Schöny, T. Pröll, H. Hofbauer. 2018. Impact of stage configurations, lean-rich heat exchange and regeneration agents on the energy demand of a multistage fluidized bed TSA CO_2 capture process. International Journal of Greenhouse Gas Control 72, 82–91. https://doi.org/10.1016/j.ijggc.2018.03.018.

[50] T.J. Tarka, J.P. Ciferno, M.L. Gray, D.J. Fauth. CO_2 capture systems utilizing amine enhanced solid sorbents. Proceedings of the 5th Annual Conference on Carbon Capture & Sequestration; Alexandria, VA, May 8−11, 2006.

Graphical abstract

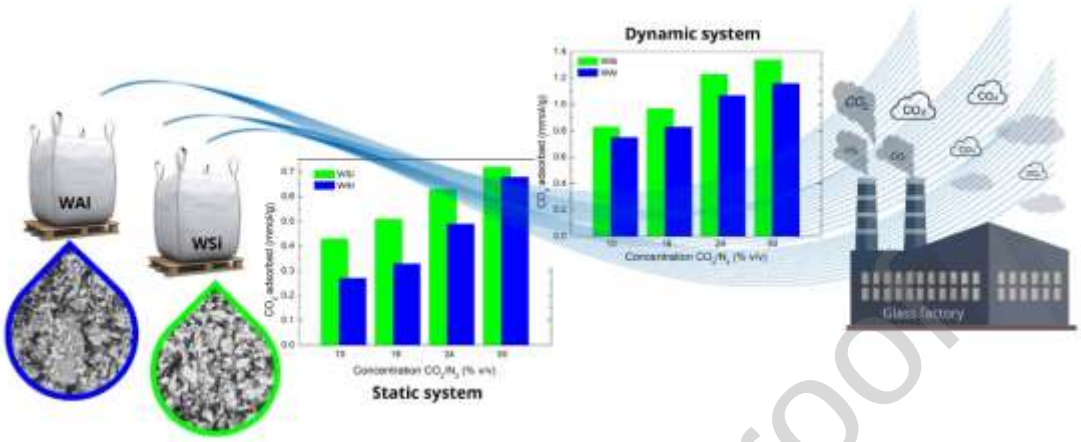

CRediT author statement

Pamela B. Ramos: Conceptualization, Methodology, Investigation, Writing-Original draft preparation

Marcelo F. Ponce. Writing-Reviewing and Editing, Investigation:

Florencia Jerez: Writing-Reviewing and Editing, Investigation, Investigation Visualization

Gastón P. Barreto: Resources, Writing- Reviewing and Editing,

Marcela A. Bavio: Resources, Visualization, Writing-Reviewing and Editing, Funding acquisition,

Declaration of interests

☒ The authors declare that they have no known competing financial interests or personal relationships that could have appeared to influence the work reported in this paper.

☐The authors declare the following financial interests/personal relationships which may be considered as potential competing interests:

Highlights

- Glass industrial wastes show good CO_2 capture capacities and good performance in successive cycles of use.
- FTIR carried out the measurement technique of the CO_2 adsorption capacity
- Static and dynamic capture systems were applied to evaluate the CO_2 adsorption.
- The CO_2 adsorption capacities of the wastes were evaluated in real flue gases demonstrating a promising projection.
- A pseudo first order kinetic for CO_2 adsorption was obtained in both wastes